Tribology International 189 (2023) 108899

Contents lists available at ScienceDirect

Tribology International

journal homepage: www.elsevier.com/locate/triboint

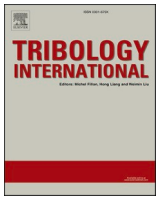

Two-dimensional structure evolution and formation of silicon carbides and diamonds in a nano-abrasion process

Piao Zhou [a], Tao Sun [b,*], Chunjin Wang [c], Hui Deng [d], Yongwei Zhu [a,**]

[a] College of Mechanical and Electrical Engineering, Nanjing University of Aeronautics and Astronautics, Nanjing 210016, China
[b] Research Center for Advanced Micro/Nano Fabrication Material, College of Chemistry and Chemical Engineering, Shanghai University of Engineering Science, Shanghai 201620, China
[c] State Key Laboratory of Ultra-precision Machining Technology, Department of Industrial and Systems Engineering, The Hong Kong Polytechnic University, Hung Hom, Kowloon, Hong Kong, China
[d] Department of Mechanical and Energy Engineering, Southern University of Science and Technology, No. 1088, Xueyuan Road, Shenzhen, Guangdong 518055, China

ARTICLE INFO

Keywords:
3D to 2D structure transition
Graphitization
Molecular dynamics simulation
3 C-SiC

ABSTRACT

Structural phase transition is often expected when crystalline substrates with high mechanical strength are processed by diamond abrasion at nanoscale. The structural evolution and formation of 3 C-SiC substrates abraded by diamond were explored using molecular dynamics simulation. The evoluted structures were derived by analyzing bond length, bond angle and coordination changes of SiC and diamond abrasives before and after nano-abrasion. Our simulation results explicitly elucidate the stable, graphene-like two-dimensional (2D) structural evolution and formation from SiC and diamond crystalline. This generolized finding of 2D structural formation from three-dimensional (3D) materials in nano-abrasion may shed light on developing new preparation options to make graphene-like 2D-SiC, which is predicted to be a chemically and mechanically stable semicondcuting material with oustanding opto-electro properties.

1. Introduction

Monocrystalline Silicon Carbide (SiC), renown for its wide band gap and mechanical, thermal stability, is widely applied in integrated circuits and power electronics [1]. To make these electronic devices, atomic-level smooth surface of SiC substrates is highly demanded. Fixed abrasive polishing (FAP) provides a highly efficient process to counter such a high surface quality challenge for SiC substrates at nanoscale [2,3]. Both the high stress and high temperature produced by FAP on SiC substrates inevitably cause the structural phase transitions of materials. A large number of nanoindentation experiments were carried out on SiC materials, and found that the SiC undergoes zincblende(ZB)-to-rocksalt (RS) [4,5] and crystalline-to-amorphous (C–A) phase transitions [6]. Molecular dynamics (MD) simulated method is then used to study abrasion and material structural phase transition mechanisms of crystalline substrates at atomic scale [7–9]. Goel [10] investigated the shear instability of 3 C-SiC during nano-cutting process, found that the pressure and shear stress induces the transition of 3 C-SiC from sp^3-SiC to sp^2-SiC by analyzing the bond angle distribution and radial distribution function of 3 C-SiC and referred the abraded out materials as the amorphous phase on the abraded SiC surface [11,12]. Wu et al. [13] reported that a ductile-regime processing of 6 H-SiC can be materialized by either C–A transition or dislocation motion during nano-abrasion process.

Most widely used SiC crystalline phases are 3 C-, 4 H-, and 6 H-SiC though there are many more other structures [14], and these crystalline phases often exist in mechanically strong and chemically stable three dimensional structures. These SiC are indirect wide band gap semiconducting materials, which makes them very valuable in green energy industry, but less ideal as opto-electronic materials because of its insufficient photon transition. Theoretical studies over past 10 years predict that a graphene-like single layered two-dimensional (2D) SiC structure is thermodynamically, mechanically and chemically stable [15–17]. The electronic properties of graphene and 2D SiC, GeC and SnC monolayers are explored by using first principle simulations. Simulation results reveal that strain in the 2D structure of group-IV carbides is the root cause for its direct band gap semicondcuting property [18], and SiC with a 2D monolayer structure has a direct band gap of 2.5 ev [19]. DFT

* Correspondence to: College of Chemistry and Chemical Engineering, Shanghai University of Engineering Science.
** Correspondence to: College of Mechanical and Electrical Engineering, Nanjing University of Aeronautics and Astronautics.
E-mail addresses: 04190006@sues.edu.cn (T. Sun), meeywzhu@nuaa.edu.cn (Y. Zhu).

https://doi.org/10.1016/j.triboint.2023.108899
Received 20 June 2023; Received in revised form 15 August 2023; Accepted 24 August 2023
Available online 25 August 2023
0301-679X/

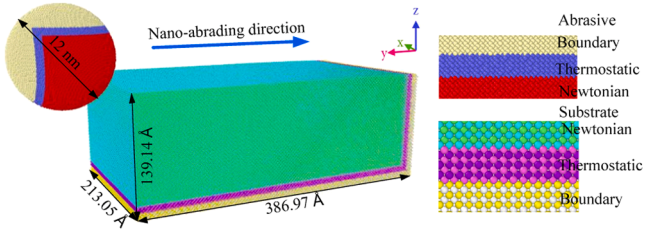

Fig. 1. Schematic representation of MD simulation model.

optimization is used to calculate and compare the most stable structures of 2D SiC monolayer compounds with different stoichiometric compositions [20], and confirms that a single layered stoichiometric 2D SiC structure is dynamically and thermally most stable. These theoretical researches inspired many experimental researchers on preparing 2D SiC in the laboratories. Lin [21] tried the solution exfoliation of 2D SiC nanoflakes with thickness of 0.5 – 1.5 nm from wurtzite SiC, and obtained some SiC sheets with a honeycomb structure. In 2021 , Sakineh Chabi's group [22] reported for the first time a successful preparation and isolation of a monolayer 2D SiC material by judiciouly controlling sonication conditions of hexagonal SiC powders in iso-propanol. Though limited in quantity, the experimental validation of 2D SiC monolayer is monumental for pursuing a most graphene-like and direct band semiconducting material that may revolutionize semiconducting material and industry.

Both Goel and our previous simulations on nano-abrasion SiC predicted the existence of SiC species with sp^2 electron configuration, but its true structure were not thoroughly investigated in details at the time. It is worth of recall that diamond tools often loose their cutting ability after being used for a period of time due to diamond graphitization in nano-cutting process [23–25]. Zhou et al. [26] investigated the wear characteristic of diamond abrasives in polishing, and reveals that graphitization wear of diamond abrasives is induced by both high temperature and high pressure. Gogotsi et al. [27,28] found that high compressive and pressure and shear stress led to graphitization and eventual amorphous transition of diamond. The critical temperature of graphitization of diamond in air and vacuum condition are reported to be 640 ℃ [29] and 1500 ℃ [30], respectively.

In this manuscript, inspired by theoretical computations and experimental observations about hard three-dimensional (3D) ceramic crystals transition to layered 2D structures of SiC and diamond and their great potentials as revolutionary semiconducting materials, both the structural evolution and end structures of the abraded SiC and debris of diamond abrasives are the focus, which may shed lights on developing novel preparation methologies of monolayer SiC 2D materials from existing 3D materials. MD simulations for investigating the structural transition characteristic of SiC and diamond in nano-abrasion are applied in our research. The evolution and formation of 2D SiC nanostructure are derived through thorough and systematic analysis of coordination number, bond length and bond angle distribution change caused by nanoabrasion. Furthermore, the critical temperature of diamond abrasives transformed from diamond into graphite structure is investigated using ABOP potential.

2. Computational details

The open source software LAMMPS is used in our MD simulation, and then the structural evolution are visualized by the OVITO software [31]. The radial distribution functions (RDFs), bond angle distribution, and coordination number of Si/C atoms before and after abrading are calculated to judge and verify whether the 2D SiC and graphite nanostructure exist or not.

In our nano-abrasion model, scales of SiC substrates are 213.05 Å, 386.97 Å, and 139.14 Å in the x, y, and z dimensions, respectively (Fig. 1). The number of atoms in a SiC substrate is 1116416. The radius of diamond abrasives is 6 nm. The abrading depth and velocity are set as 3 nm and 60 m/s respectively. Similar to traditional MD simulation of nano-cutting, the substrate is divided into boundary region, thermostatic region and newtonian region. The boundary region is used to

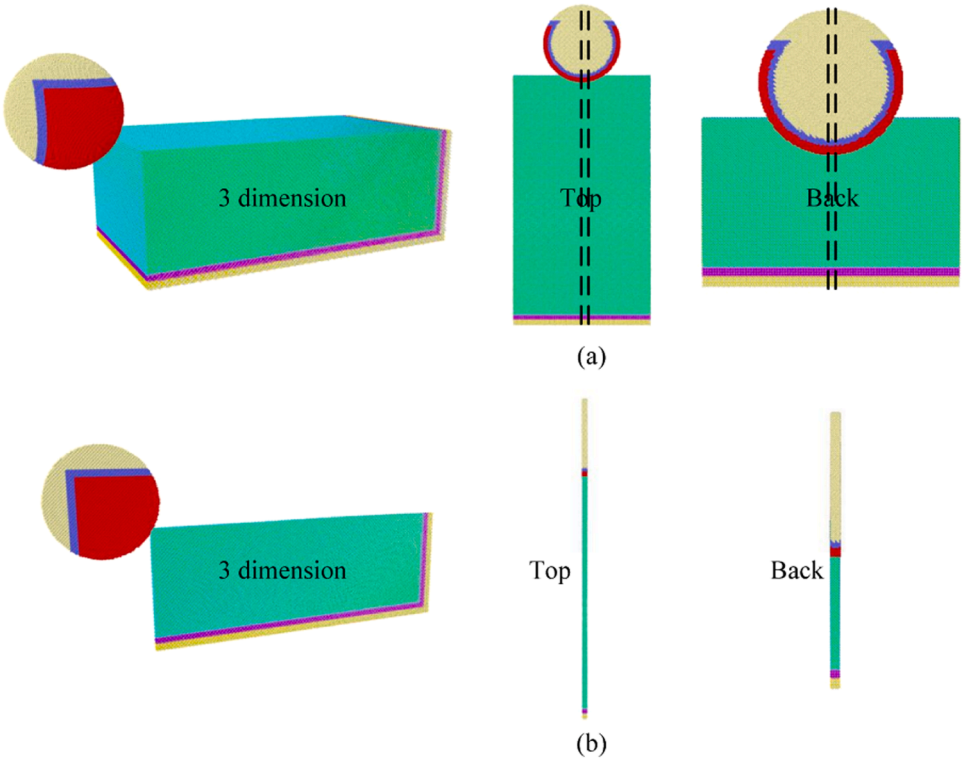

Fig. 2. The thinned 3 C-SiC (a) initial model (b) thinned to a thickness of 0.8 nm from abrasive tip.

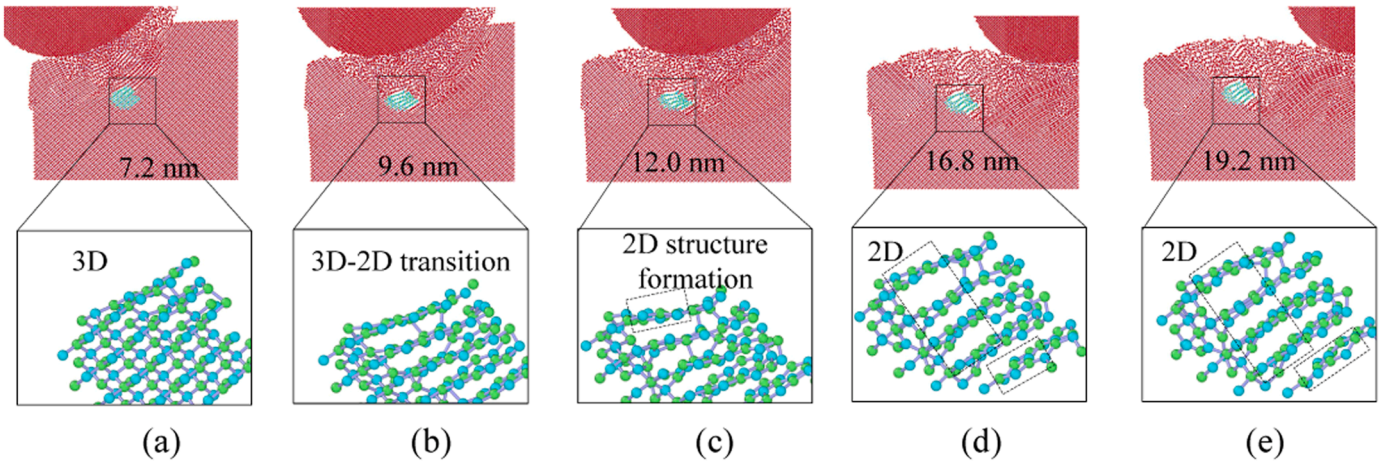

Fig. 3. Evolution and formation of 2D SiC nanostructure in 3 C-SiC during nano-abrasion process (a) 7.2 nm (b) 9.6 nm (c) 12.0 nm (d) 16.8 nm (e) 19.2 nm.

avoid any movement of SiC substrates in nano-abrasion. The thermostatic region and newtonian region contribute to equilibrate the temperature of the simulated system and calculate the structural evolution of SiC substrates, respectively.

Periodic boundary conditions are used in this simulated system to save computation time. The canonical ensemble (nvt) and microcanonical ensemble (nve) are applied in the relaxation stage with 298 K and abrading process, respectively. Potential energy functions employed in MD simulation play a very important role on the accuracy and reliability of results. ABOP potential is selected to describe interactions between Si-C, Si-Si, and C-C atoms in the whole system [32].

3. Results and discussions

3.1. Evolution and formation of 2D SiC nanostructure

In nano-abrasion, the frictional force between diamond abrasive and SiC substrates inevitably leads to increased stress and elevated temperature on the abraded substrates, which in turn affects the crystal structure and stability. Our previous study had reported an amorphous phase transition in the processed area of SiC substrates after nano-abrasion [33]. Tetrahedrally 4-coordinated Si and C atoms in 3 C-SiC substrates are partially transformed to 2-, 3-, 5- and 6-coordinated forms, predomonently 2- and 3- coordinated Si and C. The previous report mainly focused on structural phase transition of SiC in the whole abraded region, the detailed transformed nanostructure, however, was left unexamined during nano-abrading process. The highest stress and temperature of SiC substrates are localized in the frontal section of the extrusion zone when SiC is abraded by diamond crystals [33], where is most susceptible to new structural transformation. For better examing the nanostructure in selected regions, SiC substrate is sliced to a thickness of several atomic layers (0.8 nm), which is close to a two-dimensional block as illustrated in Fig. 2.

Careful examination on the magnified cross regions of Fig. 3 reveals that a thin layered 2D SiC nanostructure is formed through the abrasion process. By tracking the atomic structure of the marked region over the abrasion process, one can clearly follow the evolution process of 2D SiC nanostructure as depicted in Fig. 3a-e. In Fig. 3a, the partial 2D

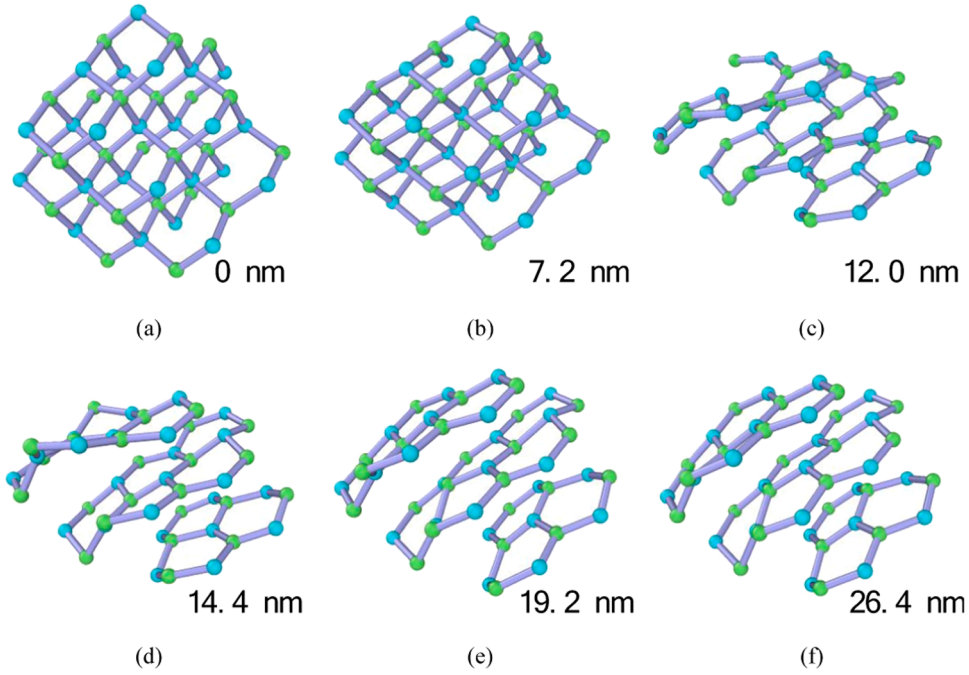

Fig. 4. 2D SiC structural configurations in nano-abrasion (a) 0.0 nm (b) 7.2 nm (c) 12.0 nm (d) 14.4 nm (e) 19.2 nm (f) 26.4 nm.

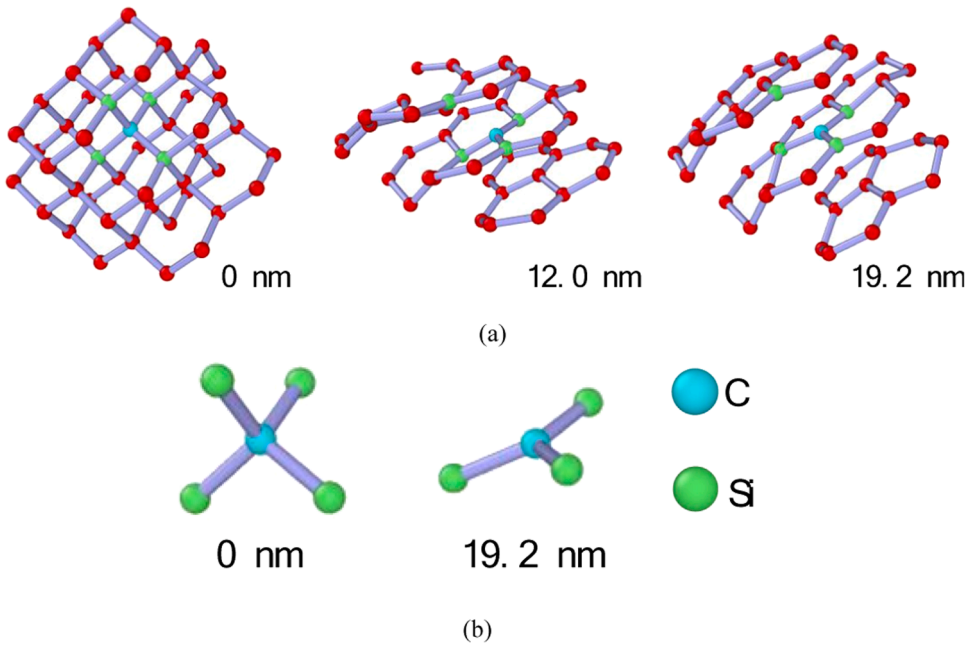

Fig. 5. Coordination structures in SiC substrates before and after nano-abrasion (a) Coordinated structures evolution (b) four-to-three coordinated structure.

nanostructure initially resides in front of diamond abrasive particle. As the diamond abrasive particle abrades forward, the partial 2D nanostructure of SiC becomes better defined, and eventually a whole piece of well developed 2D SiC sheet is observed. Be noted, the formed 2D nanostructure is stable even after the diamond abrasive abrades away from the residing position of 2D SiC nanostructure.

3.2. The bonding structure of 2D SiC

To investigate the structural phase transition of SiC substrates, bond length and bond angle are calculated and compared before and after nano-metric abrading simulation. In a 2D SiC nanostructure, the bond length between nearest Si and C atoms and bond angle of three adjacent atoms on the same layer are 1.77–1.79 Å and 120.0°, respectively [22], while the bond length and bond angle of the nearest neighboring atoms are 1.89 Å and 109.5°, respectively, in 3 C-SiC. Furthermore, the coordination numbers of Si and C atoms before and after nano-abrasion are calculated to determine whether the 2D nano-structural phase transition occurs. Both Si and C atoms are tetrahedrally 4-coordinated in 3 C–SiC. On the other hand, the 3-coordinated Si and C atoms are only present in 2D SiC nanostructure.

3.2.1. Coordination number

For better illustration of the structural evolution and formation of 2D SiC nanostructure from 3D SiC during nano-abrasion process, only a small block of SiC was presented in Fig. 4, in which one can clearly follow the step-by-step structural transformation of a tetrahedrally bonded Si-C structure in 3 C-SiC to a 2D SiC nanostructure. Initially all Si and C atoms in 3 C-SiC are tetrahedrally bonded to each other as illustrated in Fig. 4a. Under pressure and shear stress caused by cutting and sliding, the tetrahedrally bonded atomic structure is distorded as observed bond-angle deviation from ideal tetrahedral symmetry in Fig. 4b. As the diamond abrasive abrades through that prolongs the stress on the distorded SiC structure, some Si-C bonds are broken as highlighted in Fig. 4c to form vacant cavity defects. Moving along the abrading direction further, the partially damaged structure seeks to form more thermodynamically structures as showed in Fig. 4d-f. In the transformed final structure, each Si atom is bonded to three C atoms, *vice versa*, each C atom is bonded to three Si atoms arranged in a buckling monolayer plane. It is observed from Fig. 4 that the small segment of 2D

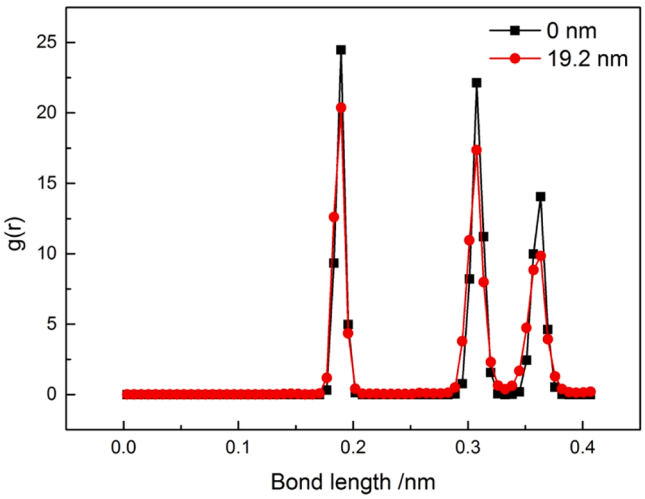

Fig. 6. RDF of 3 C-SiC substrate before and after nano-abrasion.

SiC nanostructure is slightly distorted, not like a complete plannar structure in graphene, which might be attributed to the applied high-pressure stress. The represent Si and C atoms are highlighted in green and blue, respectively, to observe the Si/C atomic evolution process of coordination numbers (Fig. 5). An outcome of four-coordinated (sp^3) to three-coordinated (sp^2) transition of Si/C atoms is essentially the formation of 2D SiC nanostructure from cubic SiC.

3.2.2. Bond length and angle

The inter-atomic distance of Si-C, Si-Si/C-C, and Si-C in 3 C-SiC are known to be 1.88, 3.07, and 3.63 Å, respectively [34]. The nearest neighboring atom distance between Si-C is 1.77–1.79 Å in 2D SiC nanostructure. The radial distribution function (RDF) in MD simulation calculates a fixed set of atomic pair distances, and can be used to characterize the structural change under pressure and shear stress. The RDFs of atoms on the SiC substrate before and after nano-abrasion are plotted in Fig. 6 to assist us to assess whether the structural transition occurs. The peak strengths of Si-C, Si-Si and C-C inter-atomic distance

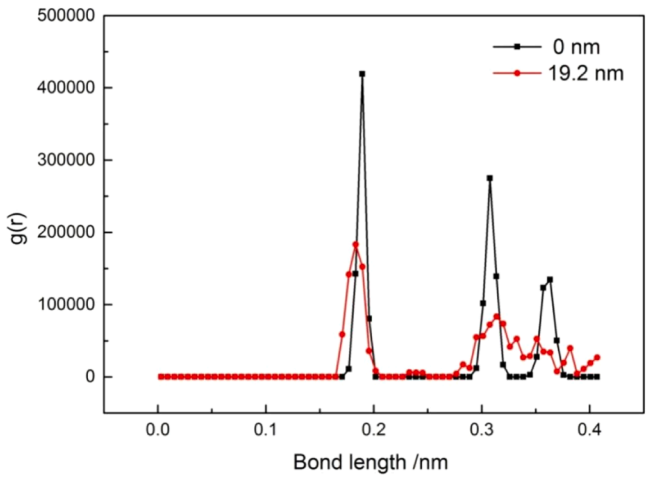

Fig. 7. RDF of 2D SiC nanostructure before and after nano-abrasion.

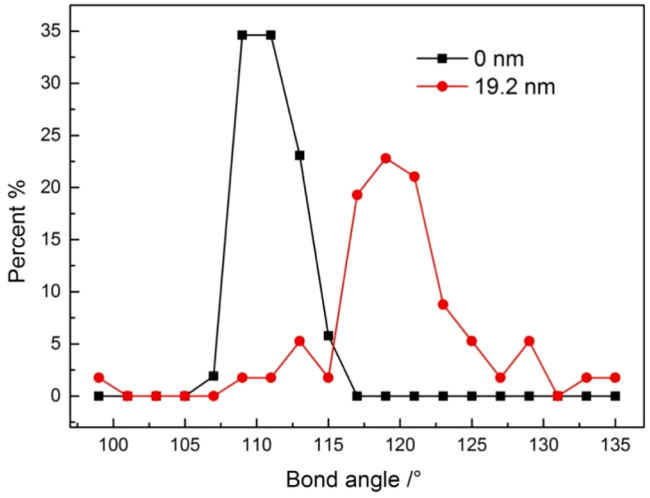

Fig. 8. Bond angle of 2D SiC nanostructure before and after nano-abrasion.

are significantly reduced after nano-abrasion, a direct evidence of a structural disorder. The RDF intensity changes of atoms undergoing 2D structural transition discussed in previous Section 3.2.1 before and after nano-abrasion are calculated and presented in Fig. 7. It is evident from Fig. 7 that the peak strength for all three inter-atomic distances is reduced, but the strength reduction that is most significant is those for C-C and Si-C inter-atomic distances, which become almost non-existent. The peak position for Si-C bond is shortened from 1.89 Å to 1.77 Å after nano-abrasion, a Si-C bond length consistent with that found in 2D SiC nanostructure. The peak positions of other two well defined Si-Si and

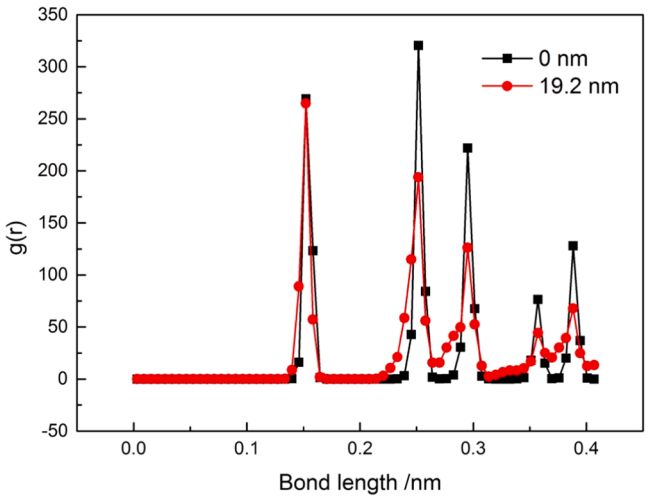

Fig. 10. RDFs of diamond abrasives before and after the nano-abrasion.

C-C distance after nanoabrasion are widely broadened with no particularly dominant structural characteristics, suggesting that Si to Si and C to C are significantly away from each other, unlike the tight and measurable distance in 3 C-SiC. These results from peak position and strength observations strongly suggest that after nanoabrasion, the 2D SiC exists as a dominant structure.

Bond angles of three adjacent atoms in a 2D structural layer and a 3D cubic structure in 3 C-SiC are well defined 120° and 109° respectively. To further support the existence of 2D SiC nanostructure after nano-abrasion, bond angle of nearest neighboring atoms that undergo 2D structural transition in our focused simulation segment are calculated (Fig. 8). Fig. 8 presents a clear picture of bond angle change from 109° to 120° before and after nanoabrasion, an undisputed support of a bonding configuration transition from sp^3-sp^3 to sp^2-sp^2 caused by surface nano-abrasion of diamond on SiC.

3.3. Critical temperature of 3 C-SiC structural transition

The formation of 2D SiC is induced by the interaction between diamond abrasives and SiC substrates in nanoabrasion which produces the processing temperature and stress. In order to obtain the influence of temperature on the formation of 2D SiC nanostructure, MD simulation is used to investigate the thermal characteristic of 3 C-SiC crystal. The NVT ensemble is used to relax the system at 298 K. Then, the temperature of 3 C-SiC crystal is raised up from 298 K to 5100 K to observe the structural evolution. ABOP potential is selected to characterize interactions between Si and C atoms in 3 C-SiC. The crystal structural evolution of 3 C-SiC with temperature is shown in Fig. 9, where blue and purple atoms represent cubic and amorphous structures, respectively. It is present that 3 C-SiC does not undergo amorphous phase transition until

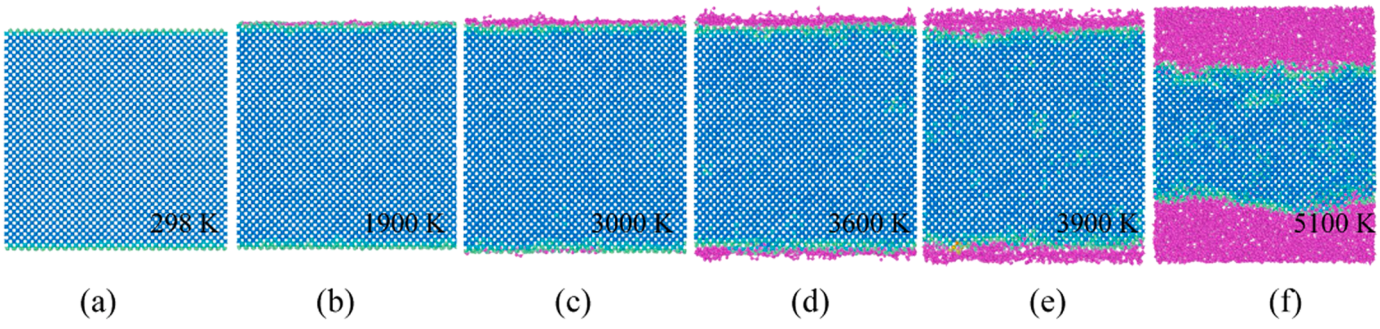

Fig. 9. Structural evolution of 3 C-SiC substrates with temperature (a) 298 K (b) 1900 K (c) 3000 K (d) 3600 K (e) 3900 K (f) 5100 K.

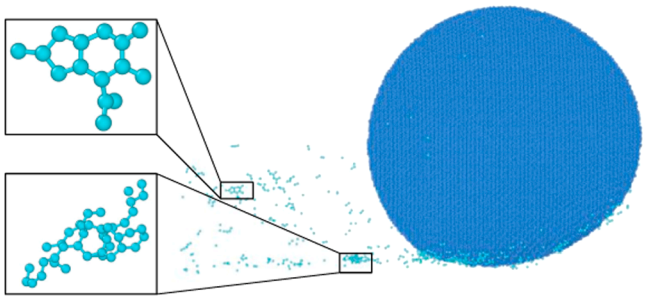

Fig. 11. Graphite-like structure in the wear-off debris from the diamond abrasive.

the temperature rise up to 3000 K. It proves the high thermodynamic stability of 3 C-SiC. However, 2D SiC nanostructure is not observed in 3 C-SiC with rising temperature. It indicates that temperature is not the main reason for inducing 2D SiC nanostructure transition during nano-abrading process. Pressure and shear stress would be the dominant factors for the formation of 2D SiC nanostructure.

3.4. Graphitized transition of diamond abrasives

We speculate that the structural transition caused by nanoabrasion should not only be found on abraded SiC but also on diamond abrasives due to Newton's law of action and reaction. A better understanding about the structural phase transition mechanism of diamond abrasives during nanoabrasion would provide a theoretical guidance for improving the application life of diamond tools.

The same analysis methodology of RDFs is applied to diamond abrasives before and after nano-abrasion is plotted. The peak strength at the inter-atomic distance of 0.154 nm is reduced about 30 % after nano-abrasion (Fig. 10). It is therefore reasonable to confirm the phase transition of diamond abrasives during nano-abrasion process.

In previous reports, diamonds would transform from unstable diamond structure to stable graphite structure when the temperature or pressure and shear stress is high enough [27,28]. Our own investigation observed a diamond-graphite phase transition of diamond abrasives in nano-abrasion [35] though the structural evolution and formation mechanism of diamond abrasives are not investigated in details. As noted in Fig. 11, graphite-like structures are found in the wear-off debris from the diamond abrasives, which are no where to be found before nano-abrasion. In order to explore diamond-to-graphite evolution process, typical graphite structures are marked in pink (Fig. 12) and orange (Fig. 13), respectively. Two mechanisms of graphite-like structural evolution are discovered. One mechanism is that a small surface section of a diamond abrasive develops a graphite-like structure caused by nanoabrasion, followed by this small segment breaking away from the abrasive surface as the diamond abrasive cuts through the SiC surface, eventually becoming a part of wear-off debris from nanoabrasion

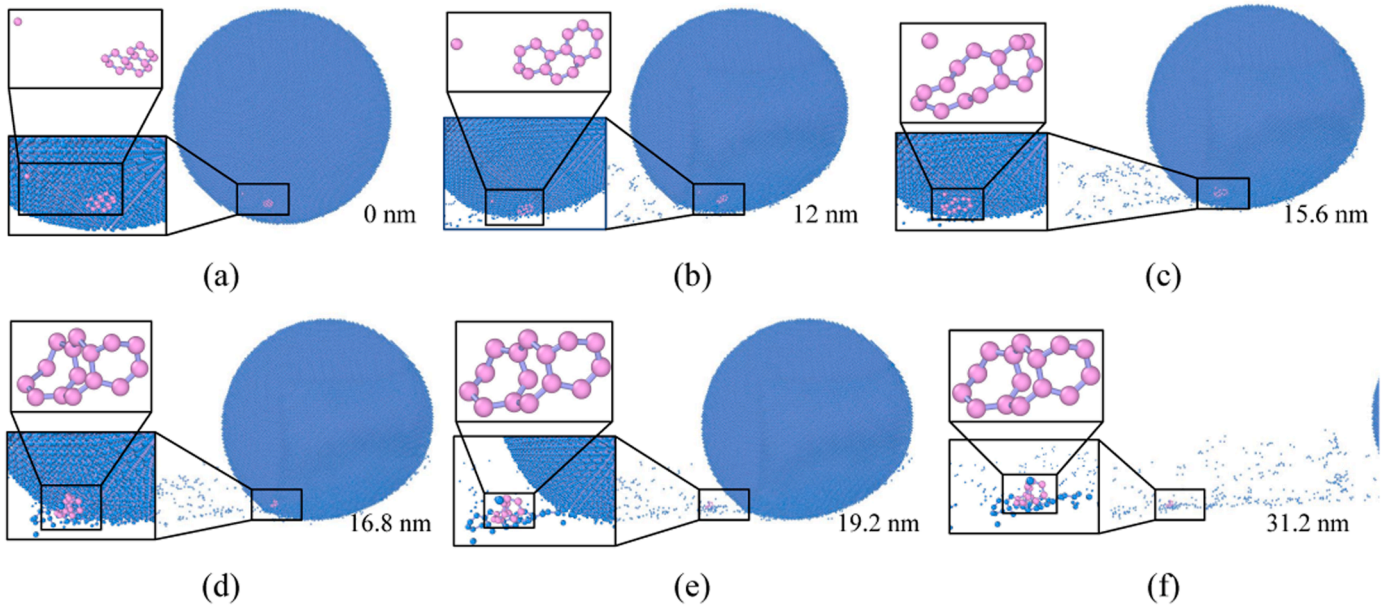

Fig. 12. Graphite-like structural evolution in diamond abrasive that breaking-off from perfect diamond structural units (a) 0.0 nm (b) 12.0 nm (c) 15.6 nm (d) 16.8 nm (e) 19.2 nm (f) 31.2 nm.

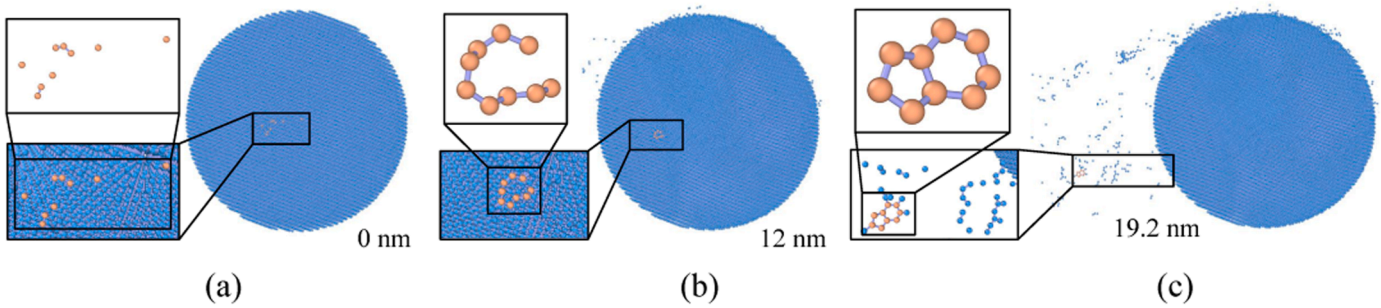

Fig. 13. Graphite-like structure in diamond abrasive that separates surface C atoms rebuilding (a) 0.0 nm (b) 12.0 nm (c) 19.2 nm.

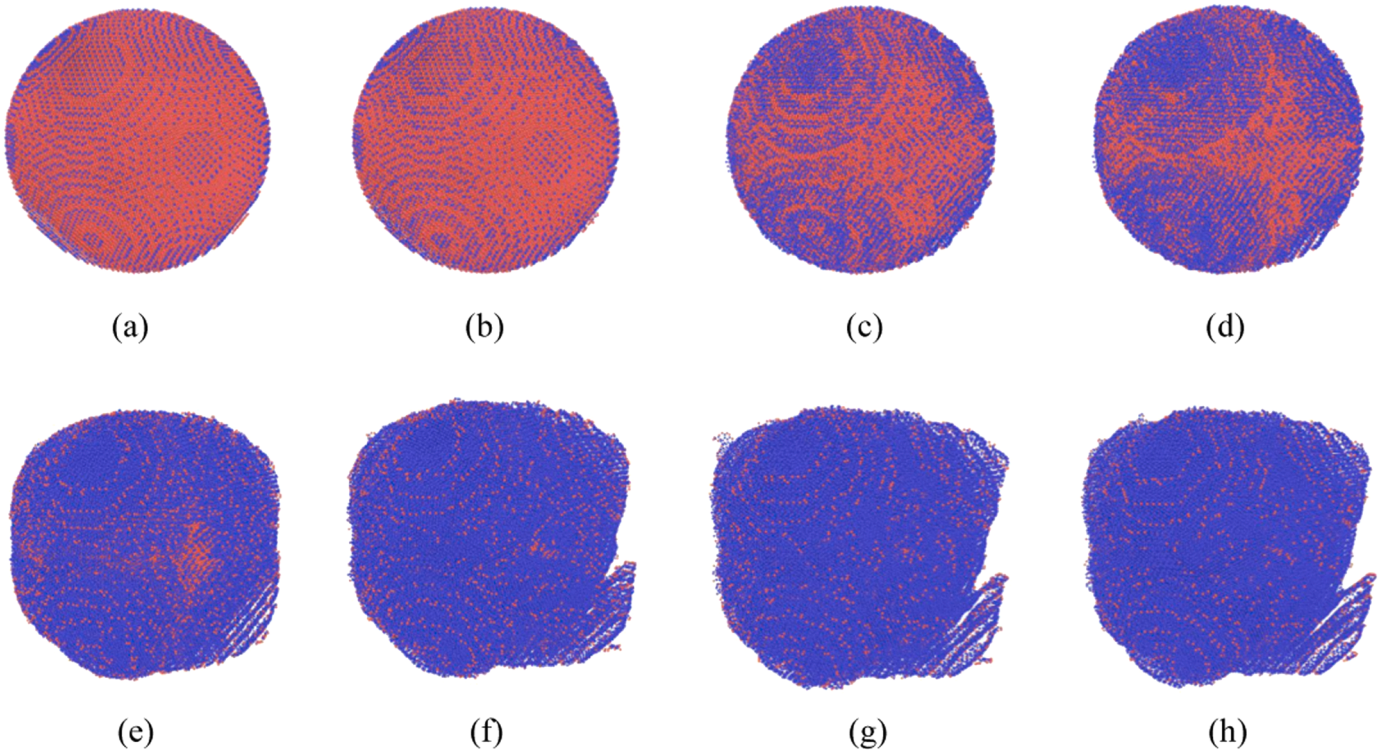

Fig. 14. Structural deformation of diamond abrasives and coordination distribution of C atoms at (a) 298 K (b) 1300 K (c) 1800 K (d) 1900 K (e) 2100 K (f) 2500 K (g) 3000 K (h) annealed to 298 K.

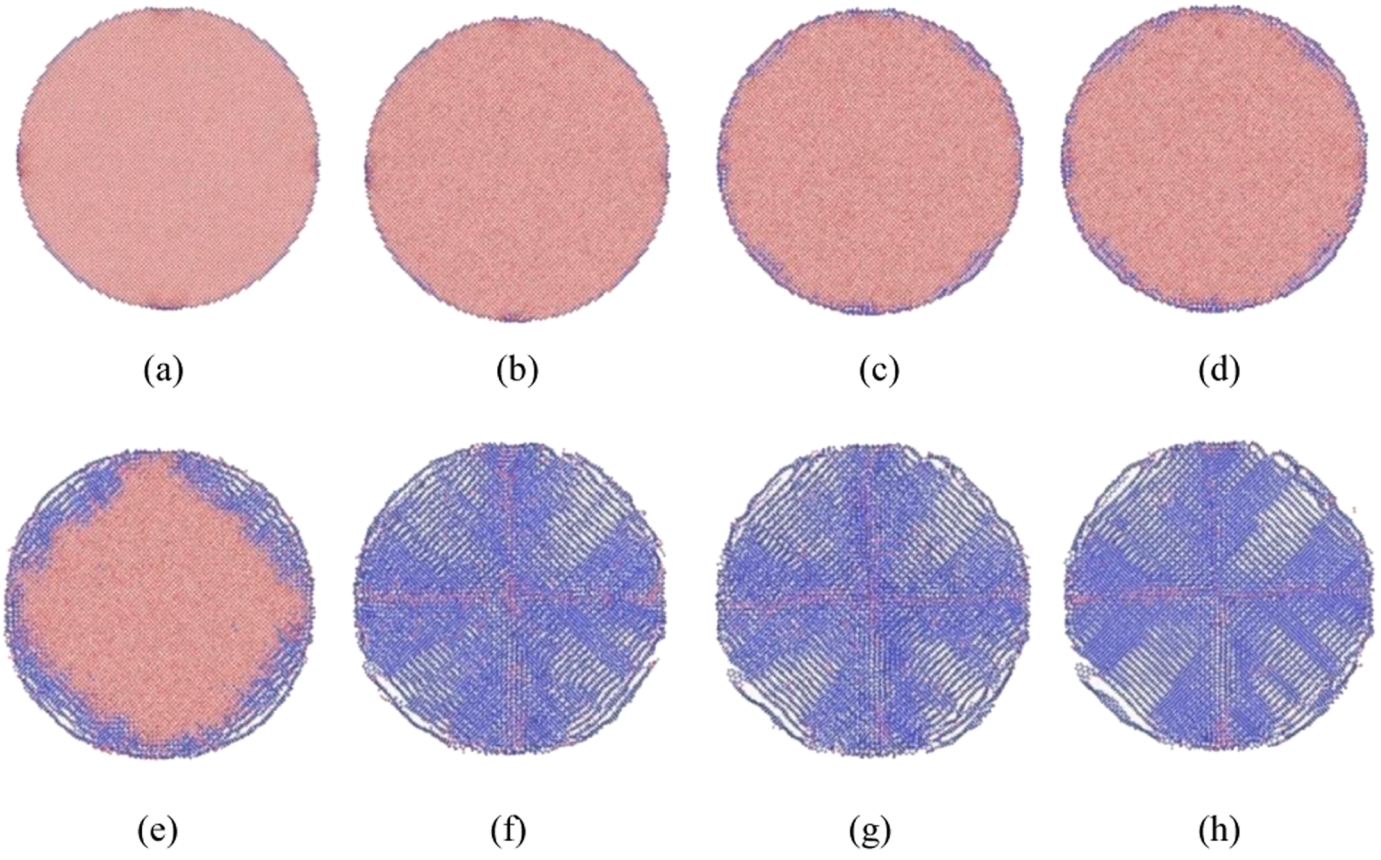

Fig. 15. The distribution of graphite atoms with temperature (a) 298 K (b) 1300 K (c) 1800 K (d) 1900 K (e) 2100 K (f) 2500 K (g) 3000 K (h) anneal to 298 K.

(Fig. 12). The other one is that C atoms are abraded off from the surface of diamond abrasives with no particularly well defined structures in Fig. 13b. These wear-off C atoms seek thermodynamic stability and then self-reconstruct to form a graphite-like structure (Fig. 13c). These graphite-like structures evolved from nanoabrasion is similar to what observed in 2D SiC structure. Different from silicon carbide crystals, two-dimensional nanostructural transition of diamond abrasives is not observed during nano-abrasion process. These observed graphitization results teach us two things: one is that a graphite-like structure can be developed from a mechanically strong and chemically stable 3D structure in a nanoabrasion process; the second, a graphite-like structure is thermodynamically preferred under temperature, pressure and shear stress.

3.5. Critical temperature of graphite structure formation

Generally, a diamond to graphite structural transition is observed at high temperature. However, diamond is also transformed into graphite at relatively low temperatures when diamond experiences high pressure and shear stress. The graphitization temperature under vacuum condition is debye temperature (1910 K) by experimental research [36]. However, the MD simulated result computed by the ABOP empirical potential is different from the experimental result. The debye temperature used as critical temperature to analyze the graphite-like transition mechanism of diamond abrasives in MD simulation would lead to incorrect results. Therefore, in order to investigate the graphitized structural transition mechanism, it is very important to obtain the critical temperature of diamond-graphite transition in our simulation.

The NVT ensemble is used to relax the system at 298 K. Then, the temperature of diamond abrasives is raised up to 3000 K to determine the critical temperature of diamond-to-graphite transition. In order to evaluate the stability of a temperature-induced graphitization of diamond abrasives, the diamond abrasives are annealed at 298 K from 3000 K. In order to obtain the critical temperature of diamond-to-graphite transition in nano-abrasion simulation, ABOP potential is selected to characterize interactions between C-C atoms in diamond.

In a graphite structure, the bond length of two adjacent atoms and bond angle of three adjacent atoms are 1.42 Å and 120°, respectively, and the corresponding bond length and bond angle in diamond structure are 1.54 Å and 109.5°, respectively. The coordination number, which is often selected to analyze the crystal structure, referring to the number of atoms in the nearest neighbor around an atom, is 4 and 3 for carbon atoms in diamonds and in graphite, respectively.

The coordination number (3 in blue and 4 in red) of C atoms at different temperature is mapped out in Fig. 14. 4-coordinated (red) C atoms dominate in diamond abrasives with 3 coordinated C atoms scattered on the surface of diamond abrasives at 298 K (Fig. 14a). As temperature is increased to 1900 K (Fig. 14d), 3-cooridnated C atoms become dominant species on diamond at 1900 K with graphite-like segment appearing in the lower right part of diamond abrasives. As temperature is further raised to 3000 K (Fig. 14g), 3 coordinated C atoms completely dominate in diamond abrasives with peeling off graphite-like segments. The diamond abrasive maintains its morphology until temperature is raised up to 2500 K (Fig. 14f), where it starts to deform from spherical particle to unregulated shape. The diamond abrasive becomes severely deformed at 3000 K in Fig. 14g, and this deformed morphology is retained when it is annealed at 298 K, suggesting that the deformed structure is stable.

A thin slice of diamond with a thickness of 3 nm is cut from the center of abrasives to track the diamond-to-graphitization evolution inside-out across diamond abrasive (Fig. 15). The 3-coordinated C atoms observed in Fig. 14a-d are mainly located on the outer layer of diamond abrasives as illustrated in Fig. 15a-d. Very slightly one can virualize a little graphite-like structure as 3-coordinated C atoms are found deeper under the outlayer at 1800 K. Graphitization of diamond from the edge to the center of the diamond abrasive is almost complete as the

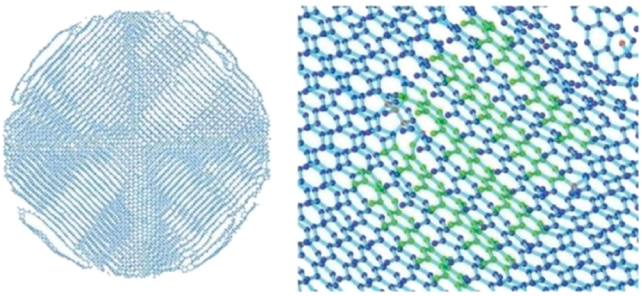

Fig. 16. The graphite structure in diamond abrasives generated from rising temperature.

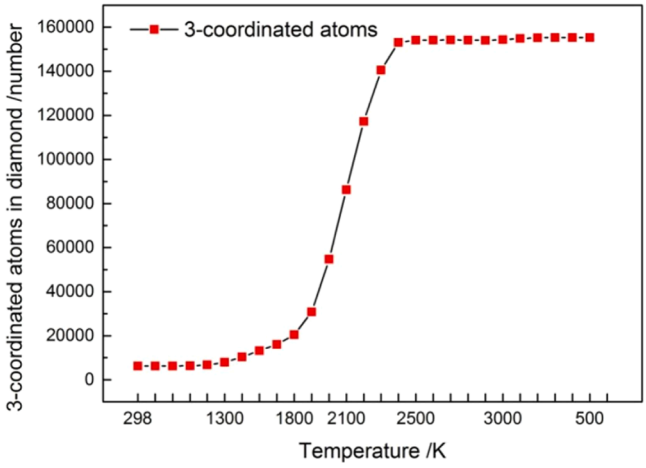

Fig. 17. Numbers of 3-coordinated C atoms in diamond abrasives *versus* temperature.

temperature reaches 2100 K with central atoms retaining a diamond structure. As the temperature continues to rise up to 3000 K (Fig. 15g), the graphite regions become better defined and expand into larger section of the particle. The transformed graphite-dominated structure is retained or better defined when it is annealed at 298 K from 3000 K, a direct evidence that a graphite structure is thermodynamically more stable than a diamond structure. Graphite structure which consists of hexagonal multilayered structure in diamond at 3000 K is presented and highlighted in green in Fig. 16. Furthermore, the total number of 3-coordinated C atoms in diamond abrasives is plotted out against temperature in Fig. 17, and shows that the number of 3-coordinated C atoms starts rising when temperature is above 1300 K, rapidly climbing at 1800 K, and reaching the highest plateau at 2500 K, consistent with observations in Fig. 15.

The temperature effect on the graphitization of diamond abrasives is further validated from quantitative analysis of the nearest C-C bond length and bond angle distribution of C atoms at varied temperatures. It can be seen from Fig. 18a that the C atoms with 1.54 Å bond length (the known bond length for diamond), represented by distribution probability, decreases while the C atoms with 1.42 Å bond length increases as the temperature rises from 298 K to 2500 K. The percentage of C atoms with a bond angle at 109°decreases almost linearly with temperature increases, while the percentage of C atoms with a bond angle at 120°increases slightly with temperature increase until temperature reaches 1900 K with a rapid rise in Fig. 18b. The near linear percentage decrease of C atoms with 109°bonding angle *versus* the rapid increase at 1900 K for C atoms with 120°bonding angle suggests that diamond structure is destructed with temperature increase while 2D structure of C atoms is not well developed and defined until temperature reaches 1900 K. One may hypothesize that the diamond structure is first being

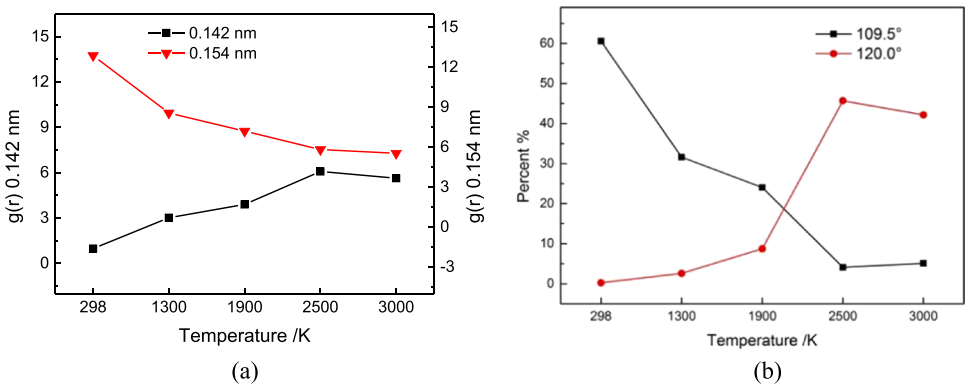

Fig. 18. The effect of temperature on the graphitization of diamond abrasives (a) bond length (b) bond angle.

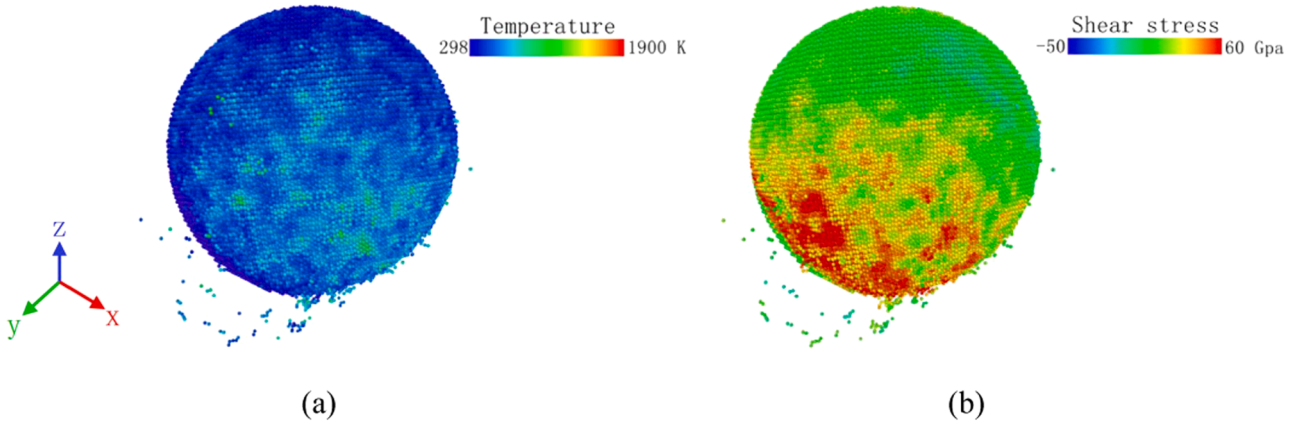

Fig. 19. The thermodynamics distribution of diamond abrasives at nano-abrading distance with 12 nm (a) processing temperature (b) shear stress.

distorted as temperature increases because the injected energy by heating leads to strong C-C bond vibration, but the diamond structure is not completely destructed. At 1900 K, there is about 50 % drop on tetrahedrally coordinated C atoms while there is only 10 % of C atoms with hexagonal structure, suggesting the existence of large amount of C atoms with no well defined structures. As temperature further increases, thermodynamic driving force transforms the partially destructed diamond structure into more stable hexagonal 2D structure. Furthermore, the phenomenon of diamond-to-graphitization transition with rising temperature is proved by previous experiments [37].

3.6. Graphitization transition factors

Our MD simulated result reveals that the diamond-graphite transition takes place with high temperature (T > 1900 K). However, diamond also can be transformed into graphite when the ideal shear stress is high enough (S>95 GPa) [38]. As shown in Fig. 19, the maximum abrading temperature generated at the edge of the diamond abrasive is not enough to cause graphitization. The highest local shear stress is close to the critical shear stress with diamond-graphite transition. Different from temperature and stress, separately, induce the diamond-graphite phase transition, the structural phase transition of diamond abrasives are affected by thermodynamic coupling effect during nano-abrading process. The interatomic thermal vibration enhance in diamond abrasives due to the higher processing temperature, which induce the weakening of the bonding strength and soft of diamond abrasives [39]. The stress is released in diamond with high temperature. The coupling effect of processing temperature and stress would induce to decrease the critical temperature and shear stress of diamond-graphite transition, which are the main factors for diamond-to-graphitization transition during nanoabrading process.

4. Summary

Molecular dynamics simulation is used to gain extensive insights into the structural phase transition of 3 C-SiC and diamond monocrystalline in nano-abrasion process. After careful analysis of removed debris, one can clearly visualize the evolution process of a transformed 2D SiC nanostructure in 3 C-SiC nano-abrasion process. The bond length and bond angle with nearest atoms of 3 C-SiC are transformed from 1.89 Å to 1.77 Å, and from 109° to 120° in the newly formed 2D nanostructure, respectively, under nano-abrasion stress. The tetrahedrally 4-coordinated Si and C atoms are transformed to 3-coordinated Si and C atoms when cubic-2D transition occurs, which present sp^3-sp^2 transition.

MD simulation result also shows that the critical temperature of diamond-to-graphite transition is 1900 K by using ABOP potential. The diamond structure experiences structural distortion, followed by structural destruction, and eventually transform into a thermodynamically stable graphite structure when temperature rises up to 1900 K and beyond. There exist two transformation mechanisms of a graphite-like structure from a diamond structure in nano-abrasion. One is that a new graphite-like structure is formed from reconstruction of removed surface C debris of diamond abrasives. The other one is that surface C atoms with diamond structure directly breaks off from perfect diamond structural units. The couple effects of temperature and shear stress are the main factor for diamond-to-graphitization transition in nano-abrasion.

Our MD simulation result signifies an outstanding contribution of pressure and shear stress to the structural transformation from well defined tetrahedrally 4-cooridinated 3D structure to well defined

triganganolly 3-coordinated 2D structure, and the later structure is thermodynamically more stable. These result provides us options on making 2D materials with graphene-like structure, specifically a new broad band semiconducting 2D SiC with graphene-like structure.

Statement of originality

I confirm that this paper is original and it has not been published previously and it is not under consideration elsewhere.

Declaration of Competing Interest

The authors declare that they have no known competing financial interests or personal relationships that could have appeared to influence the work reported in this paper.

Data availability

Data will be made available on request.

Acknowledgements

This work was supported by the National Natural Science Foundation of China (Grant Nos. 52075318), the Joint Funds of the National Natural Science Foundation of China (Grant Nos. U20A20293).

References

[1] Xu M, Girish YR, Rakesh KP, Wu P, Manukumar HM, Byrappa SM, et al. Recent advances and challenges in silicon carbide (SiC) ceramic nanoarchitectures and their applications. Mater Today Commun 2021;28:102533.
[2] Luo Q, Lu J, Tian Z, Jiang F. Controllable material removal behavior of 6H-SiC wafer in nanoscale polishing. Appl Surf Sci 2021;562:150219.
[3] Luo Q, Lu J, Xu X. Study on the processing characteristics of SiC and sapphire substrates polished by semi-fixed and fixed abrasive tools. Tribol Int 2016;104:191–203.
[4] Mishra M, Szlufarska I. Possibility of high-pressure transformation during nanoindentation of SiC. Acta Mater 2009;57:6156–65.
[5] Shimojo F, Ebbsjö I, Kalia RK, Nakano A, Rino JP, Vashishta P. Molecular dynamics simulation of structural transformation in silicon carbide under pressure. Phys Rev Lett 2000;84:3338–41.
[6] Gogotsi YG, Kailer A, Nickel KG. Phase transformations in materials studied by micro-Raman spectroscopy of indentations. Mater Res Innov 1997;1:3–09.
[7] Zhou Y, Huang Y, Li J, Zhu F. Effect of water film on the nano-scratching process of 4H-SiC under the constant load. Tribol Int 2022;175:107802.
[8] Bi G, Li Y, Lai M, Fang F. Mechanism of polishing lutetium oxide single crystals with polyhedral diamond abrasive grains based on molecular dynamics simulation. Appl Surf Sci 2023;616:156549.
[9] Wu Z, Zhang L, Yang S, Wu C. Effects of grain size and protrusion height on the surface integrity generation in the nanogrinding of 6H-SiC. Tribol Int 2022;171:107563.
[10] Goel S. Shear instability of nanocrystalline silicon carbide during nanometric cutting. Appl Phys Lett 2012;100:535–8.
[11] Meng B, Yuan D, Xu S. Coupling effect on the removal mechanism and surface/subsurface characteristics of SiC during grinding process at the nanoscale. Ceram Int 2019;45:2483–91.
[12] Yin Z, Zhu P, Li B, Xu Y, Li R. Atomic simulations of deformation mechanism of 3c-sic polishing process with a rolling abrasive. Tribol Lett 2021:69.
[13] Wu Z, Liu W, Zhang L. Revealing the deformation mechanisms of 6H-silicon carbide under nano-cutting. Comput Mater Sci 2017;137:282–8.
[14] Saurav Goel. The current understanding on the diamond machining of silicon carbide. J Phys D Applied Phys 2014;47:243001.
[15] Wei G. New stable two dimensional silicon carbide nanosheets. J Alloy Compd Interdiscip J Mater Sci Solid-State Chem Phys 2021:868.
[16] Herrero CP, Ramírez R. Quantum effects in two-dimensional silicon carbide. J Phys Chem Solids 2022;171:110980.
[17] Martins NF, Fabris GSL, Albuquerque AR, Sambrano JR. A new multifunctional two-dimensional monolayer based on silicon carbide. FlatChem 2021;30:100286.
[18] Tie-Yu Lü, Xia-Xia Liao, Hui-Qiong Wang, Jin-Cheng Zheng. Tuning the indirect–direct band gap transition of SiC, GeC and SnC monolayer in a graphene-like honeycomb structure by strain engineering: a quasiparticle GW study. J Mater Chem 2012;22:10062–8.
[19] Lin X, Lin S, Xu Y, Hakro AA, Hasan T, Zhang B, et al. Ab initio study of electronic and optical behavior of two-dimensional silicon carbide. J Mater Chem C 2013;1:2131–5.
[20] Li P, Zhou R, Zeng XC. The search for the most stable structures of silicon–carbon monolayer compounds. Nanoscale 2014;6:11685–91.
[21] Lin SS. Light-emitting two-dimensional ultrathin silicon carbide. J Phys Chem C 2012;116:3951–5.
[22] Chabi S, Guler Z, Brearley AJ, Benavidez AD, Luk TS. The creation of true two-dimensional silicon carbide ER. Nanomaterials 2021;11:1799.
[23] Zong W, Zhang J, Liu Y, Sun T. Achieving ultra-hard surface of mechanically polished diamond crystal by thermo-chemical refinement. Appl Surf Sci 2014;316:617–24.
[24] Goel S, Luo X, Reuben RL. Molecular dynamics simulation model for the quantitative assessment of tool wear during single point diamond turning of cubic silicon carbide. Comput Mater Sci 2012;51:402–8.
[25] Goel S, Luo X, Reuben RL, Rashid WB. Atomistic aspects of ductile responses of cubic silicon carbide during nanometric cutting. Nanoscale Res Lett 2011;6:589.
[26] Zhou Y, Huang Y, Li J, Zhu F. The effect of contact types on SiC polishing process. Mater Sci Semicond Proc 2022;147:106709.
[27] Gogotsi YG, Kailer A, Nickel KG. Pressure-induced phase transformations in diamond. J Appl Phys 1998;84:1299–304.
[28] Gogotsi YG, Kailer A, Nickel KG. Materials Transformation of diamond to graphite. Nature 1999;401:663–4.
[29] Xu NS, Chen J, Deng SZ. Effect of heat treatment on the properties of nano-diamond under oxygen and argon ambient. Diam Relat Mater 2002;11:249–56.
[30] Evans T, James PF. A study of the transformation of diamond to graphite. Proc R Soc Lond Ser A Math Phys Sci 1964;277:260–9.
[31] Stukowski Alexander. Visualization and analysis of atomistic simulation data with OVITO–the Open Visualization Tool. Model Simul Mater Sci Eng 2010;18:2154–62.
[32] Erhart P, Albe K. Analytical potential for atomistic simulations of silicon, carbon, and silicon carbide. Phys Rev B 2005;71:35211.
[33] Zhou P, Zhu Y, Sun T, Lin L, Li J, Wang Z, et al. Stress-induced structural phase transition of 3C–SiC with TLK structure in a nano-abrading process. Mater Sci Semicond Proc 2020;112:104893.
[34] Liu Y, Li B, Kong L. Molecular dynamics simulation of silicon carbide nanoscale material removal behavior. Ceram Int 2018;44:11910–3.
[35] Zhou P, Sun T, Shi X, Li J, Zhu Y, Wang Z. Atomic-scale study of vacancy defects in SiC affecting on removal mechanisms during nano-abrasion process. Tribol Int 2020;145:106136.
[36] Butenko YV, Kuznetsov VL, Chuvilin AL, Kolomiichuk VN, Stankus SV, Khairulin RA, et al. Kinetics of the graphitization of dispersed diamonds at “low” temperatures. J Appl Phys 2000;88:4380–8.
[37] O’Bannon E, Xia G, Shi F, Wirth R, King A, Dobrzhinetskaya L. The transformation of diamond to graphite: experiments reveal the presence of an intermediate linear carbon phase. Diam Relat Mater 2020;108:107876.
[38] Cohen ML, Roundy D. Ideal strength of diamond, Si, and Ge. Phys Rev B 2001;64:212103.
[39] Nguyen V, Fang T. Phase transformation and subsurface damage formation in the ultrafine machining process of a diamond substrate through atomistic simulation. Sci Rep 2021;11:17795.